

History matching of petroleum reservoirs using deep neural networks

Rasim Alguliyev, Ramiz Aliguliyev, Yadigar Imamverdiyev, Lyudmila Sukhostat *

Institute of Information Technology, Azerbaijan National Academy of Sciences 9A, B. Vahabzade Street, Baku AZ1141, Azerbaijan



ARTICLE INFO

Keywords:

History matching
AlexNet
Bi-directional gated recurrent unit
Variational autoencoder
Permeability
Porosity

ABSTRACT

This paper proposes a novel approach based on deep learning to improve oil reservoirs' history matching problem. Deep autoencoders are widely used to solve the oil industry problems. However, as the input data increases, the autoencoder parameters increase exponentially. Our model is based on a convolutional variational autoencoder using AlexNet and bi-directional gated recurrent units. It parameterizes large-scale oilfield reservoirs. The proposed model is integrated into an ensemble smoother with multiple data assimilation to perform history matching. The proposed approach is validated on two reservoir models: PUNQ-S3 and Volve field. The root mean squared error, R^2 , and mean absolute error are calculated to verify the effectiveness of the proposed approach. The results show that the proposed model can effectively study the complex geological features of oil fields and be used in expert systems for reservoir modeling.

1. Introduction

According to [Oliver et al. \(2008\)](#), history matching is an inverse problem that plays a key role in reservoir design for assessing reservoir properties (porosity, permeability, etc.).

History matching adapts the model to reproduce the past. Besides, it helps in forecasting. It reduces the risks involved and allows experts to make decisions.

It is necessary to match the production history or compare real and measured data with the predicted values to check the quality of the reservoir model. In the case of coincidence, the model is considered suitable for forecasting. It can be obtained quickly enough, but the model selection is a lengthy process requiring clarification. Comparing the observed features of the reservoir behavior with the typical indicators can be used to estimate the input values (porosity, permeability, and others).

History assimilation allows checking the formation modeling quality of new wells by comparing the measured pressure with the predicted pressure at the point of oil well drilling. The quality of the model is confirmed according to geological, geophysical, and field data. In the petroleum literature, history matching is known as an incorrect inverse problem with non-unique solutions ([Ma, 2019](#)).

Currently, the uncertainty of the reservoir model parameters allows a quantitative and qualitative assessment of the forecast ([Gilman and](#)

[Ozgen, 2013](#)). Several historical matching models are often generated to evaluate the parameters' uncertainty. However, creating an ensemble of historical-comparable models that can reproduce the observable historical data of a real reservoir leads to a correct estimate of uncertainty ([Tavassoli et al., 2004](#)). Despite the constructed model quality, the dynamics of production may affect the behavior of the reservoir in a different way than was predicted.

In traditional historical matching, BHP (bottom hole pressure), WOPR (well oil production rate), and WCT (water cut) are used. Geological models that reflect the structure and petrophysical parameters do not often consider the production data. In turn, hydrodynamic models that reflect dynamic properties often only approximate the geological structure.

Recently, ES (ensemble smoother) ([van Leeuwen and Evensen, 1996](#)), EnKF (ensemble Kalman filter) ([Evensen, 1994](#)), and their modifications have gained popularity. Besides, ensemble methods can generate several reservoir implementations that include geophysical measurements and production data that quantify the uncertainty of the associated model.

Ensemble-based iterative smoothing agents ([Emerick and Reynolds, 2013; Luo et al., 2015; Chen and Oliver, 2014; Stordal and Lorentzen, 2014](#)) have become the preferred approach to assist the history matching of reservoir properties. Smoothers assimilate all data in one update step and avoid complex and lengthy restarts of the reservoir

Abbreviations: PORO, Porosity; GOR, Gas-oil ratio; PERMX, Horizontal permeability; PERMZ, Vertical permeability; NTG, net-to-gross; OWC, Oil-Water Contact; MULTZ, multipliers for vertical permeability; BHP, bottom-hole pressure; BiGRU, bi-directional gated recurrent unit.

* Corresponding author.

E-mail address: lsuhostat@hotmail.com (L. Sukhostat).

<https://doi.org/10.1016/j.iswa.2022.200128>

Received 6 April 2022; Received in revised form 28 August 2022; Accepted 19 September 2022

Available online 23 September 2022

2667-3053/© 2022 The Author(s). Published by Elsevier Ltd. This is an open access article under the CC BY-NC-ND license (<http://creativecommons.org/licenses/by-nc-nd/4.0/>).

Table 1
Summary of history matching methods.

Refs.	Proposed approach	Main contribution	Reservoir model	Geostatistical parameters
Lorentzen et al. (2019)	A method based on acoustic impedance and production data	<ul style="list-style-type: none"> Automatic adaptation Reduces data mismatch 	Norne field	PORO; PERMX; NTG; OWC; MULTZ; k_{rw} ; k_{rg} ; PORO; PERMX; PERMZ.
Verga et al. (2013)	Improved sampling algorithm	Reduction of forecast uncertainty	PUNQ-S3	
Zhang et al. (2016)	History assimilation of non-Gaussian fields	The resulting posterior model is highly consistent with the reference model	PUNQ-S3	PORO; PERMX; PERMZ; k_{rw} ; k_{ro} ; Reservoir saturation; Aquifer. PERMX; PERMZ.
Canchumuni et al. (2019)	Parameterization using CVAE and ES	ES-MDA based parameterization for large data	2 × 2D synthetic cases 3D synthetic case	2 × 2D synthetic cases 3D synthetic case
Li and Yang (2012)	Parameters estimation using ensembles	Petrophysical parameters estimation	PUNQ-S3	Gas saturation; Oil saturation; k_{rw} ; k_{ro} ; k_{rg} ; PORO; PERMX; PERMZ.
Kim et al. (2019)	Field optimization using COMPSO	Low computational cost	2D synthetic case PUNQ-S3	PORO; PERMX; PERMZ.
Liu et al. (2019)	Parameterization based on PCA and CNN	Significant uncertainty reduction for existing wells	2 × 2D synthetic cases	PORO; PERMX; PERMZ.
Canchumuni et al. (2017)	ES-MDA-DL for facies models	Deep generative models based on a autoencoder architecture were used to reconstruct facies models	PUNQ-S3	PORO; PERMX; PERMZ.
Ranazzi and Sampaio (2019a)	ES-MDA ensemble size evaluation for history matching	A good reduction for various ensemble sizes.	UNISIM-I-H	PORO; NTG; PERMX; PERMZ; OWC; MULTZ; Rock compressibility; k_{rw} ; Corey exponent.
Canchumuni et al. (2018)	Parameterization based on DBNs integrated with ES-MDA	Better than ES-MDA	2 × 2D synthetic cases; Brugge field.	2 × 2D synthetic cases; Brugge field.
Rana et al. (2018)	GP-VARS for uncertainty quantification	Uncertainty quantification results better than EnKF	PUNQ-S3	PORO; PERMX; PERMZ.
Hajizadeh et al. (2011)	Ant colony optimization based history matching	Uncertainty bands reduction in produced cumulative oil forecasting	Teal South model (Gulf of Mexico); PUNQ-S3	PERMX; PERMZ; Rock compressibility; Aquifer. PORO; PERMX; PERMZ; NTG.
Ranazzi and Sampaio (2019b)	Kalman gain localization in ES	Data mismatch reduction not considering localization	UNISIM-I-H	PORO; PERMX; PERMZ; NTG.
Negash et al. (2017)	Proxy modeling and multiobjective optimization for history assimilation	Fast prediction of uncertain reservoir parameters	PUNQ-S3	PORO; PERMX; PERMZ; MULTX; MULTY; MULTZ.
Isaiah et al. (2013)	Neural network based reservoir simulation	Time reduction	Fort Collins field (Colorado, US)	PORO; PERMX; PERMZ.
Mohamed et al. (2010)	History assimilation using PSO	Preserving static data from wells	Brugge field	PORO; PERMX; PERMZ; NTG.

(continued on next page)

Table 1 (continued)

Refs.	Proposed approach	Main contribution	Reservoir model	Geostatistical parameters
Chen and Oliver (2010)	An ensemble-based optimization	<ul style="list-style-type: none"> Localization alleviates the effect of spurious correlations. Covariance inflation compensates for the insufficiency of the ensemble variability Updating of global parameters reduces the tendency for overshoot. 	Brugge field	PORO; PERMX; PERMZ; NTG; Water saturation; OWC; k_{rw} ; k_{ro} ; BHP.
Liu and Grana (2018)	ES-MDA based reservoir models optimization	Convolutional autoencoder can sparsely represent the data using spatial patterns.	2D synthetic case	PORO; PERMX; PERMZ.
Kim et al. (2021)	Iterative learning-based many-objective history matching using deep neural network with stacked autoencoder	<ul style="list-style-type: none"> A methodology to upgrade the empirical correlations made by deep neural network. Considers the observed dynamic data with equal weights. 	PUNQ-S3	PORO; PERMX; PERMZ.
Mohd Razak and Jafarpour (2020)	CNNs for feature-based model calibration under uncertain geologic scenarios	<ul style="list-style-type: none"> It can be used in real time to map flow response data to reservoir property distribution. The workflow can be used as “black-box” inversion proxy model. 	2 × 2D synthetic cases; 3D synthetic case; Volve field.	PORO; PERM.

simulator. However, the problem with ensemble methods is that false correlations between parameters are inevitable with a limited ensemble size. This problem increases with the size of the parameter space and the number of observations. It leads to unrealistic updates to the model parameters and underestimation of the posterior error of covariance (Furrer and Bengtsson, 2007). ES-MDA (Ensemble Smoother with Multiple Data Assimilation) (Emerick and Reynolds, 2013) is used to optimize reservoir models using production data. ES calculates a global update while avoiding restarting the simulation from the initial time step every time new data is assimilated. ES-MDA is an iterative version of ES that is suitable for handling non-linear cases. An ensemble is updated iteratively, repeatedly assimilating data with inflated covariance to achieve better data matching.

The development of computing power in recent years has led to an increase in the application of artificial neural networks (ANN) based methods to various tasks, such as solar air heater modeling (Esen et al., 2008a), analysis of heat pump systems performance (Esen et al., 2008b; 2008c; 2009; 2017), oil production forecasting (Nikitin et al., 2022), etc.

The approach based on deep variational autoencoder (VAE), a powerful tool, is widely used in various applications (Ju et al., 2018; Chen et al., 2018; Feng and Duarte, 2018). It is used to generate and fine-tune the porosity and permeability parameters of the reservoir model. It is applied to generate and fine-tune the porosity and permeability parameters of the reservoir model.

In this paper, deep learning is applied to the history matching problem. Convolutional variational autoencoder based on the bi-directional GRU (gated recurrent unit) model (ConvBiGRU-VAE) is proposed for generating permeability and porosity parameters using ES-MDA. The method is implemented on the PUNQ-S3 and Volve reservoir models.

The rest of the paper is organized as follows. Section 2 describes a literature review. The proposed approach for history matching is presented in Section 3. Section 4 describes the experimental reservoir models. Evaluation metrics are presented in Section 5. The experimental results are given in Section 6. In Section 7 the obtained results are discussed. Conclusions are given in Section 8.

2. Related work

The section analyses state-of-the-art works on history matching (Table 1). A large number of researches on reservoir history matching are associated with ensemble Kalman filter (EnKF) (Evensen, 1994; Evensen, 2003).

Chen and Oliver (2010) considered the EnKF method for a large-scale

reservoir model. Covariance localization, covariance inflation, and regularization are used to improve the model. Also, the simultaneous estimation of the reservoir parameters was considered (Lo and Yang, 2012). The accuracy increased using three-phase relative permeability curves. Besides, the improved strength Pareto evolutionary algorithm (SPEA2) was implemented (Verga et al., 2013).

Emerick and Reynolds (2013) proposed ES-MDA to increase computational efficiency and work with Big data.

An adaptive method of localization based on distance was developed (Ranazzi and Sampaio, 2019a). A direct relationship was established between model mismatches and the critical length used in localization.

The adaptive methodology (Emerick, 2016) was reviewed to assess ensemble size (Ranazzi and Sampaio, 2019b). The work shows that the ensemble size affects the number of iterations and the selected inflation factors. Smaller ensemble sizes of 100 and 300 showed worse results in comparison with the ensemble size equal to 500. The approach allows determining the importance of the correct choice of ensemble size given the available computing resources.

Methods based on genetic algorithms, such as PCA (principal component analysis), have found application in parameterization (Mohamed et al., 2010). The PSO method was then applied to find the possible parameter combinations matching historical data. Also, a stochastic search method for multiple history matching models generation based on ant colony optimization was considered (Hajizadeh et al., 2011). The method's advantages include the efficiency and ease of navigation in high-dimensional search spaces. This work studied the influence of additional data points on history matching and forecast uncertainty. Kim et al. (2019) developed COMPSO (cooperative micro-particle swarm optimization) for high-dimensional and complex issues in field development. The computational efficiency was improved.

The use of proxy modeling is considered. An approach applies MOGA (multiobjective genetic algorithm) and MOGAA (multiobjective genetic goal attainment algorithm) to misfit functions (Negash et al., 2017). A new approach that uses Gaussian processes (GP) and variogram analysis of response surface (VARS), also known as GP-VARS, was proposed (Rana et al., 2018). Probabilistic evaluation of reservoir properties and estimate ultimate recovery (EUR) were obtained.

In (Lorentzen et al., 2019), an approach was proposed for reservoir data assimilation. The method successfully reduces data mismatch of seismic data instead of just looking at production data.

A hybrid approach that combines the neural network with a kriging algorithm was developed (Isaiah et al., 2013). The experimental results showed that the process could reduce computational time by decreasing

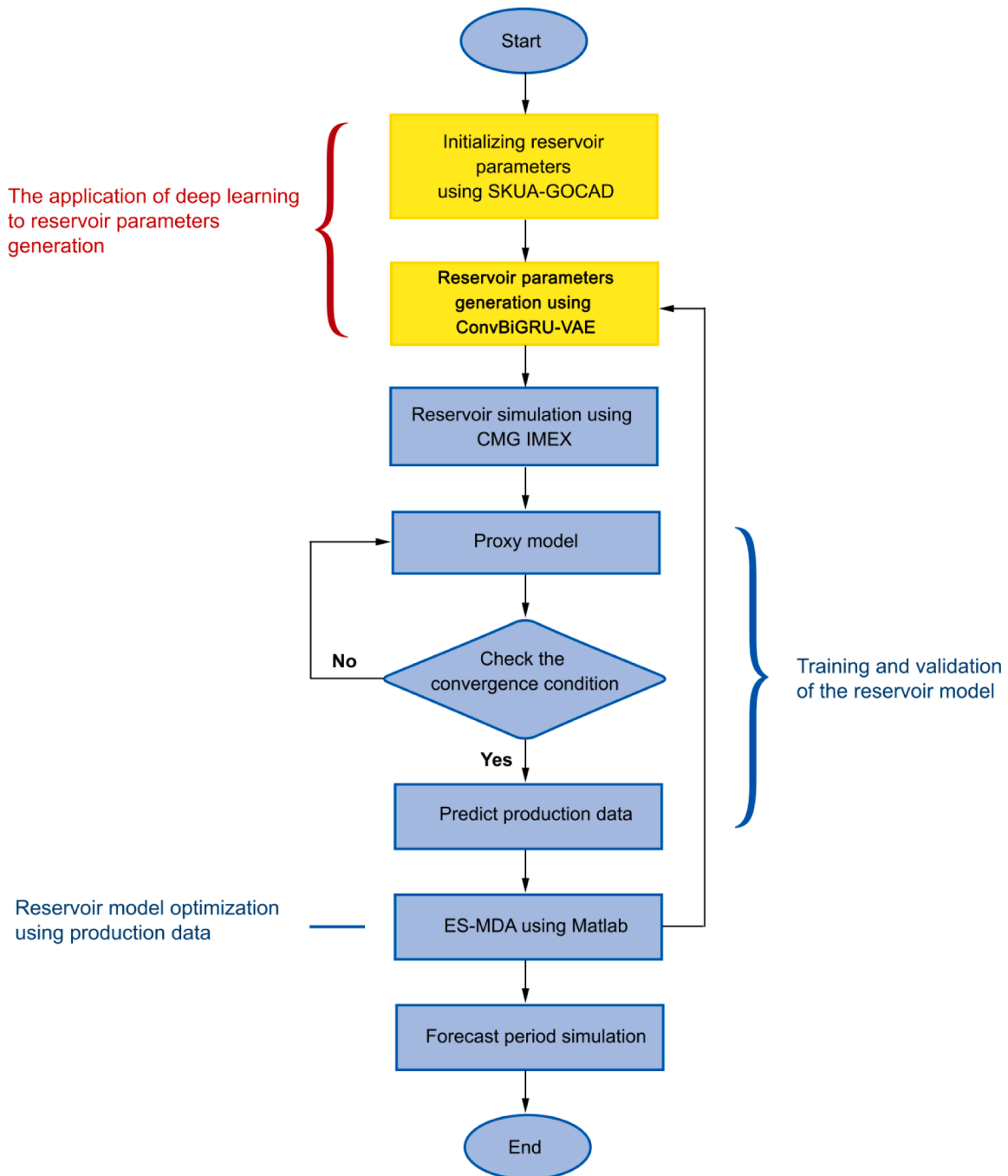


Fig. 1. Flowchart of the proposed approach.

the number of steps in the algorithm. A parameterization of geological facies using DBN (deep belief networks) as an autoencoder was developed (Canchumuni et al., 2018). In turn, using the decoder reconstructs the facies after each ES-MDA iteration.

Liu and Grana (2018) described convolutional autoencoder-based data parametrization. ES-MDA is applied to update the prior ensemble. The results obtained using seismic data in the model significantly improve the reservoir simulation process.

Zhang et al. (2016) proposed a two-stage procedure to preserve the facies structures to increase the precision of history matching. The first stage consists of facies distribution inversion to get formation characteristics. Then the history matching to continuous petrophysical

parameters sampling was performed based on the posterior values.

A method based on deep learning for history matching (ES-MDA-DL) was developed (Canchumuni et al., 2017) to increase the stability of parameterization. The re-parameterization of geological images in terms of coefficients following Gaussian distributions was carried out. Parameterization using PCA and truncated Gaussian (ES-MDA-PCA) was also proposed in the paper. The ES (ensemble smoother) method was considered to assimilate geological and production data (Canchumuni et al., 2019). CVAE was used to parameterize facies in reservoir models.

An approach using CNN (convolutional neural network) with PCA was considered for the low-dimensional geological models' parameterization using multipoint spatial statistics (Liu et al., 2019). A metrics set

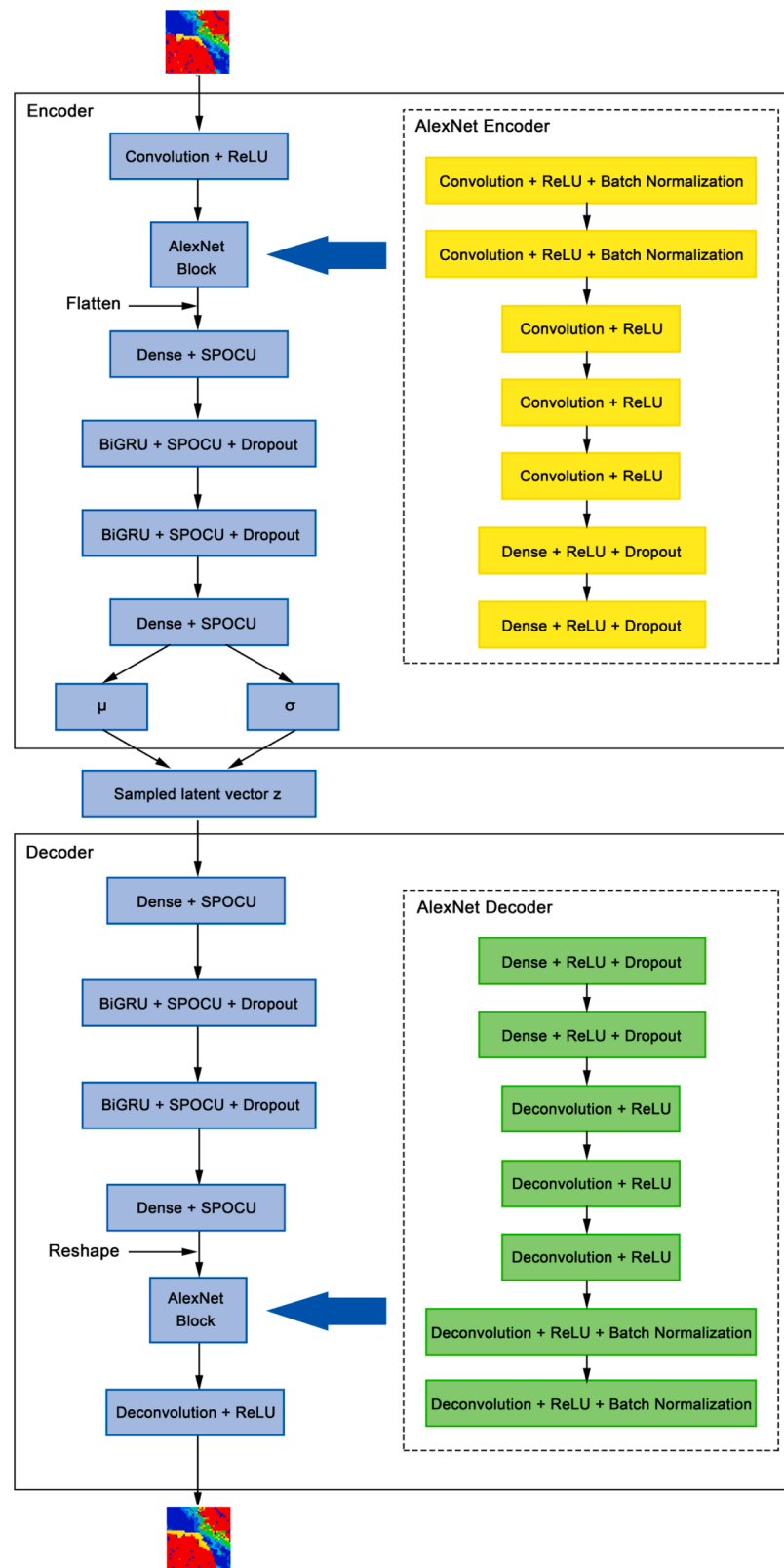


Fig. 2. The architecture of convolutional BiGRU-VAE.

based on CNN describes multiple point correlations that allow preserving the complex geological patterns in the reference model.

Summarizing the above works, we propose the ConvBiGRU-VAE model for the oil reservoir history matching task. Using the observed data, the aim is to generate and select the most accurate reservoir model

parameters for each grid cell from the posterior distribution.

3. Proposed approach

This study aims to assess reservoir geology's impact on the simulated

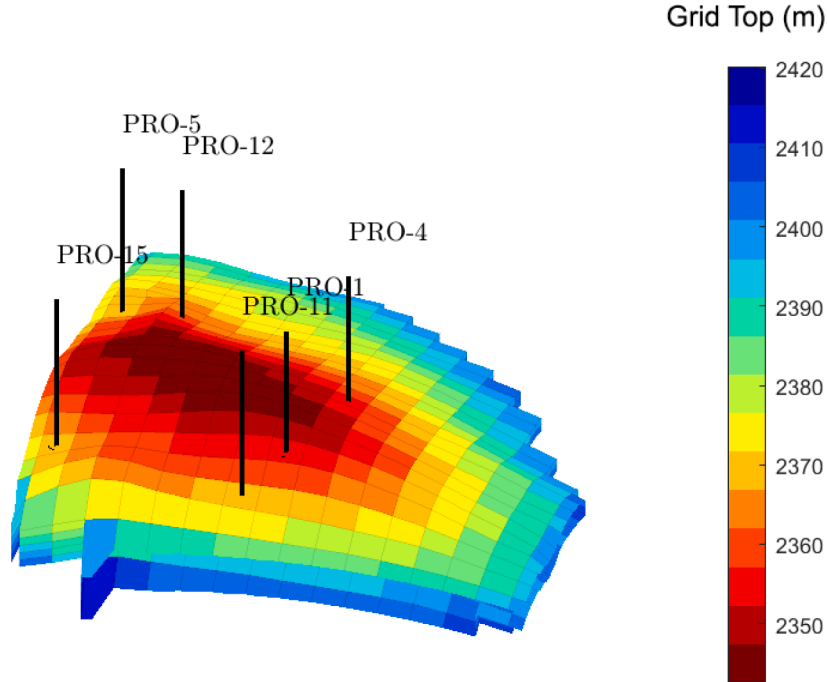


Fig. 3. PUNQ-S3 reservoir model.

Table 2
PUNQ-S3 reservoir well locations.

Location	Layer	Well name	Well type
(10,22)	4,5	PRO-1	producer
(9,17)	4,5	PRO-4	producer
(17,11)	3,4	PRO-5	producer
(11,24)	3,4	PRO-11	producer
(15,12)	4,5	PRO-12	producer
(17,22)	4	PRO-15	producer

Table 3
Reservoir model parameters for PUNQ-S3.

Variable	Description
Phases	Water/Oil/Gas
Grid system	$19 \times 28 \times 5$
Reservoir thickness	15 m
Rock porosity	0.01 to 0.30
Horizontal permeability	5 to 995 mD
Vertical permeability	3 to 498 mD
Reference pressure	23446 kPa
Reference depth	2355.00 m
Reservoir temperature	220 °F
Oil density	912 kg/m ³
Gas density	0.8266 kg/m ³
Water density	1000 kg/m ³
Water-Oil contact	2395 m
Gas-Oil contact	2355 m
Rock compressibility	4.5e-6 1/kPa

model's considered parameters. The flow diagram of the proposed approach is presented in Fig. 1.

The main features of the proposed deep learning based approach are

as follows:

- Deep ConvBiGRU-VAE, which includes the convolution layers in the encoder and decoder parts of VAE, generates images of reservoir parameters.
- The prior models' dynamic and static data are used to train the proposed approach.
- Posterior models are generated using ConvBiGRU and VAE to improve the speed of posterior model sampling.
- The SPOCU activation function is used for the new fully connected and BiGRU layers.

ConvBiGRU is applied to find the relation between the a priori models' latent features and the corresponding production data.

- History matching error for the production well is evaluated using the root mean square error (RMSE), R-squared (R^2), and mean absolute error (MAE) metrics as described in Section 5.

In the first step, various geological realizations are created. Different parameters (such as porosity, permeability, etc.) are taken from the CMG CMOST software data file to make geological realizations using the SKUA-GOCAD software. Deep ConvBiGRU-VAE is used to generate and fine-tune the parameters.

The porosity φ and logarithmic values of horizontal ($\ln(k)$) and vertical permeability ($\ln(k_v)$) are considered static parameters:

$$m_j = [\varphi_1, \varphi_2, \dots, \varphi_N, \ln(k)_1, \ln(k)_2, \dots, \ln(k)_N, \ln(k_v)_1, \ln(k_v)_2, \dots, \ln(k_v)_N]_j^T, \quad (1)$$

where N is the number of cells and j is the number of the ensemble member.

Production data is calculated for each model based on a reservoir fluid flow simulator. The observed data are WOPR (well oil production rate), GOR (well gas-oil ratio), and BHP (well bottom-hole pressure):

$$d_{obsj} = [WOPR_1, WOPR_2, \dots, WOPR_{N_w}, BHP_1, BHP_2, \dots, BHP_{N_w}, GOR_1, GOR_2, \dots, GOR_{N_w}]_{obsj}^T, \quad (2)$$

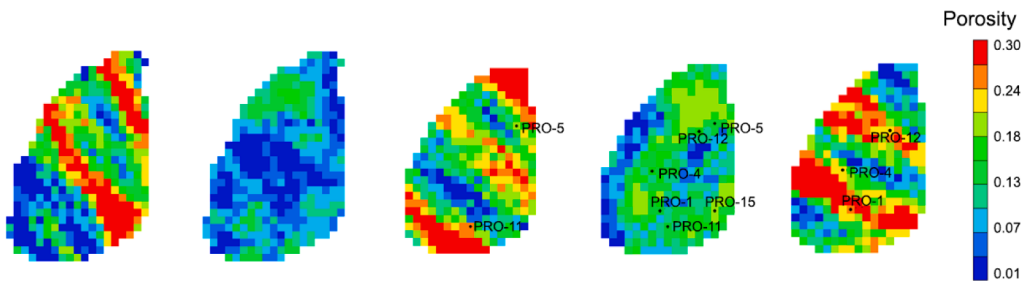
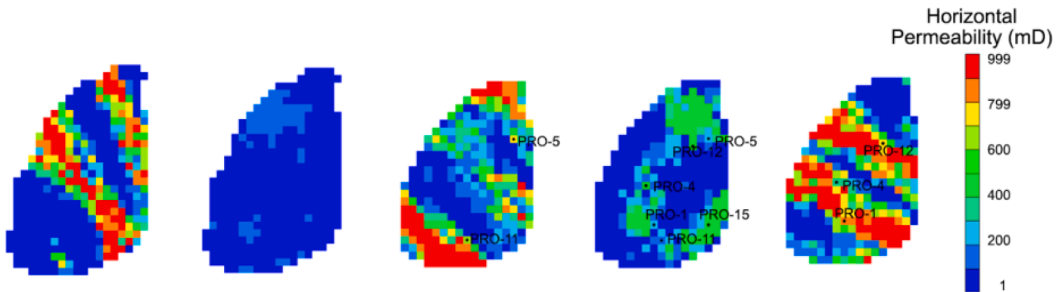
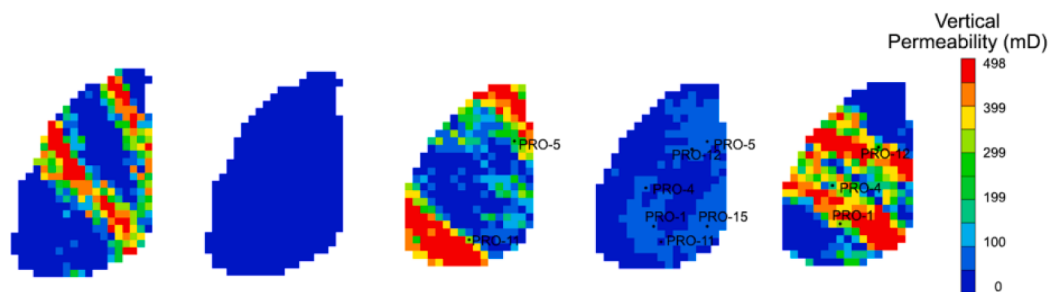
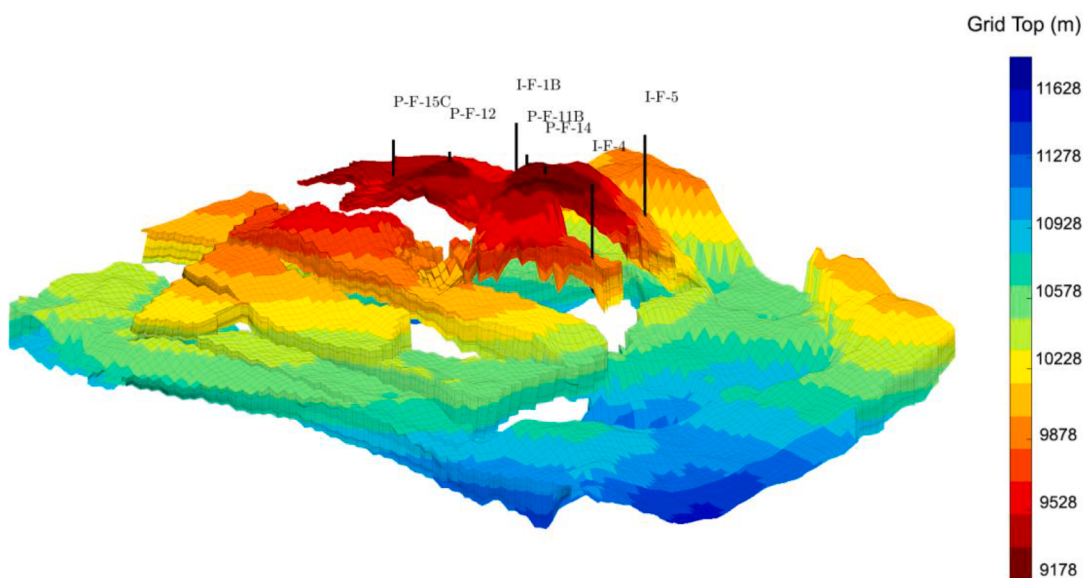
**Fig. 4.** Porosity for PUNQ-S3 reservoir model.**Fig. 5.** Horizontal permeability for PUNQ-S3 reservoir model.**Fig. 6.** Vertical permeability for PUNQ-S3 reservoir model.**Fig. 7.** Volve field model.

Table 4
Volve field well locations.

Location	Layer	Well name	Well type
(65,48)	1-63	P-F-14	producer
(60,37)	3-61	P-F-12	producer
(69,53)	1-22	P-F-15D	producer
(80,36)	1-14	P-F-11B	producer
(57,51)	6-63	P-F-1C	producer
(84,41)	1-63	I-F-5	injector
(73,28)	1-63	I-F-4	injector
(66,58)	6-63	I-F-1B	injector

Table 5
Reservoir model parameters for the Volve field.

Variable	Description
Phases	Water/Oil/Gas
Grid system	19 × 28 × 5
Reservoir thickness	60 m
Rock porosity	0.10 to 0.26
Horizontal permeability	10 to 500 mD
Vertical permeability	10 to 800 mD
Reference pressure	329 psi
Reference depth	5000 m
Reservoir temperature	230 °F
Oil density	882 kg/m³
Gas density	1.0989 kg/m³
Water density	1052 kg/m³
Water-Oil contact	3200 m
Gas-Oil contact	500 m
Rock compressibility	0.00002 1/psi

where N_w is the number of wells in the reservoir model.

At each step, new distributions of porosity and permeability are generated. CMG IMEX produces reservoir simulations based on these realizations. The proxy reservoir model is then trained and validated using CMG CMOST commercial software. The ES-MDA algorithm is used to update the reservoir model.

The number of ensemble implementations is a compromise between the computational cost and the quality of the solution. The

implementation error falls when the number of ensemble members grows. However, the limitation is that an assessment of each element is necessary at each stage of history matching.

These steps allow the evaluation of the reservoir model and predict future production rates. It is an iterative process that achieves a fit between historical and simulated data.

The proposed approach is an effective tool for generating and fine-tuning the reservoir model parameters, which could be used in expert decision-making.

3.1. Convolutional BiGRU-VAE

The paper proposes deep ConvBiGRU-VAE, which includes the convolution layers in the encoder and decoder parts of VAE, to generate images of reservoir parameters. The general structure of the proposed ConvBiGRU-VAE model is presented in Fig. 2.

VAE is an autoencoder in which the encoder evaluates hidden variables from the reservoir model parameters, and the decoder restores static parameters from the hidden variables.

ConvBiGRU-VAE includes an AlexNet-based block combined with BiGRU layers. We use AlexNet (Krizhevsky et al., 2012) to extract features from images. The considered AlexNet model consists of seven layers: five are convolutional, and two are fully connected. We used the SPOCU activation function in this network for the new fully connected and BiGRU layers.

The SPOCU activation function (Kiselák et al., 2021) is used to increase the robustness of the proposed model:

$$G(x) = \rho H\left(\frac{x}{\gamma} + \xi\right) - \rho H(\xi), \quad (3)$$

where $\xi \in (0, 1)$, $\rho, \gamma > 0$ and

$$H(x) = \begin{cases} r(c), & x \geq c \\ r(x), & x \in [0, c] \\ 0, & x < 0 \end{cases} \quad (4)$$

with $r(x) = x^3(x^5 - 2x^4 + 2)$ and $1 \leq c < \infty$. According to (4), we consider $c = \infty$, $\rho = 3.0937$, $\xi = 0.6653$ and $\gamma = 4.437$.

Also, pooling layers are considered to reduce the dimension of the

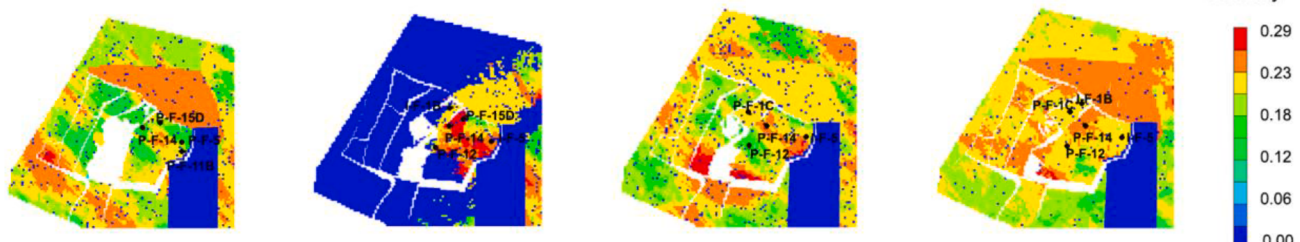


Fig. 8. Porosity of the Volve field model.

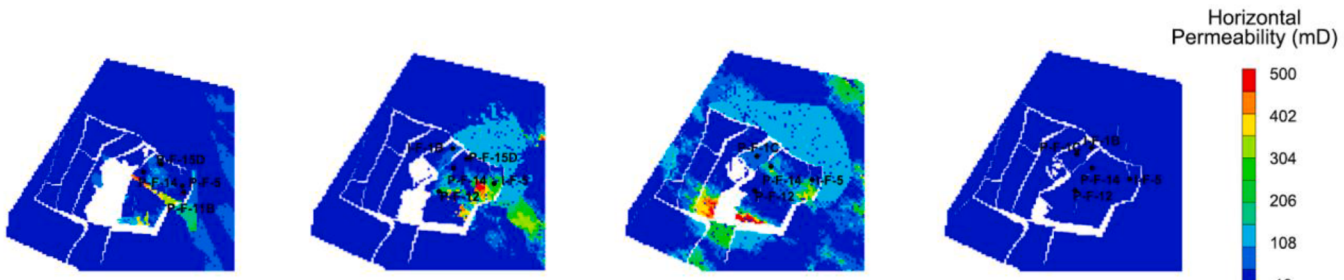


Fig. 9. Horizontal permeability of the Volve field model.

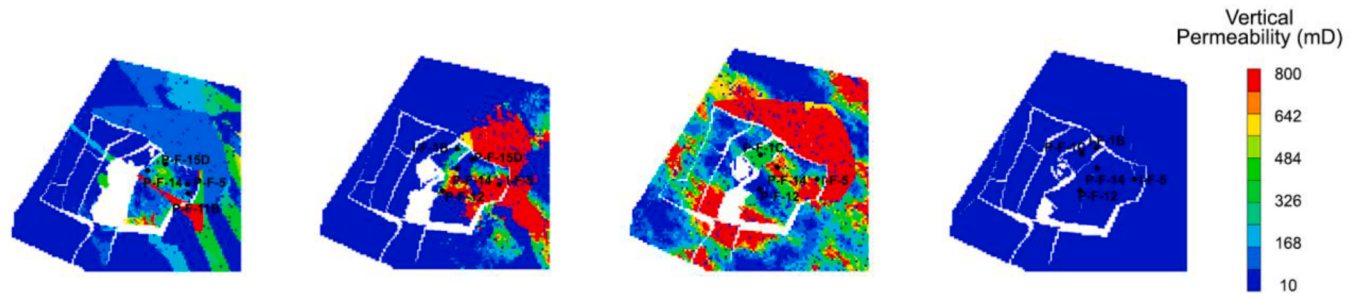


Fig. 10. Vertical permeability for Volve field model.

convolutional layers. The Dropout and Batch Normalization layers are added to prevent overfitting. Each of the layers of the network is responsible for different image features. Deepening into the network, the features acquire their uniqueness for the considering problem.

BiGRU includes two GRU layers (Gao et al., 2022): forward output GRU and reverse output GRU.

The GRU layers units are calculated as follows (Cho et al., 2014):

$$z_t^{GRU} = \sigma(W_z[h_{t-1}^{GRU}, F_t^{GRU}]), \quad (5)$$

$$r_t^{GRU} = \sigma(W_r[h_{t-1}^{GRU}, F_t^{GRU}]), \quad (6)$$

$$y_t^{GRU} = (1 - z_t^{GRU}) \circ h_{t-1}^{GRU} + z_t^{GRU} \circ \tanh(W_t^{GRU} \circ h_{t-1}^{GRU}, F_t^{GRU}), \quad (7)$$

where z_t^{GRU} is an update gate, y_t^{GRU} is an output of GRU, r_t^{GRU} is a reset gate, $\{F_1^{GRU}, F_2^{GRU}, \dots, F_T^{GRU}\}$ is a feature vector, h_{t-1}^{GRU} are the hidden states, and W_z , W_r and W are the weight matrices.

At each moment, there is input to two GRUs in opposite directions, and the output is jointly determined to make the result more accurate (Gao et al., 2022). The BiGRU output is as follows

$$H = \overrightarrow{y_t^{GRU}} \oplus \overleftarrow{y_t^{GRU}}, \quad (8)$$

where $\overrightarrow{y_t^{GRU}}$ and $\overleftarrow{y_t^{GRU}}$ are two GRUs, and \oplus is the addition element.

Let x be the vector of observation variables, z be the latent vector, and ψ and θ are the sets of encoder and decoder parameters, respectively. The observation vector x is introduced into the encoder, at the output of which the mean value $\mu_\psi(x)$ and the variance $\sigma_\psi^2(x)$ are obtained. They are used for sampling the latent vector (Nishizaki, 2017).

z is sampled after the Gaussian distribution with $\mu_\psi(x)$ and $\sigma_\psi^2(x)$ (Kingma and Welling, 2014, 2015). The decoder $p_\theta(z|x)$ generates x from z . Then $\mu_\psi(x)$ and $\sigma_\psi^2(x)$ are directly evaluated to generate the output vector x .

Gradients are calculated based on $p_\theta(x)$:

$$\partial p_\theta(x) = \int p_\theta(z)p_\theta(x|z)dz. \quad (9)$$

$p_\theta(x)$ can be approximated using the stochastic encoder $q_\psi(z|x)$ as follows:

$$\log p_\theta(x) = L_{\theta,\psi} + KL(q_\psi(z|x) \| p_\theta(z|x)). \quad (10)$$

Moreover, the second term in (10) is Kullback-Leibler (KL), which is not negative, and the first is the variational lower bound that can be defined as

$$L_{\theta,\psi} = \log p_\theta(x) - KL(q_\psi(z|x) \| p_\theta(z|x)) \leq \log p_\theta(x). \quad (11)$$

After that, we use a decoder network based on BiGRU and AlexNet to solve the oil well history matching problem.

3.2. ES-MDA

The ES-MDA method is used in this paper for model optimization using production data. For the task of reservoir history matching, unknown parameters (porosity, permeability, etc.) for each member of the ensemble j have the form:

$$m_j = [m_{1j}, m_{2j}, \dots, m_{N_m j}]^T \in R^{N_m}, \quad (12)$$

where N_m is the number of parameters.

Simulated and observed data (for example, WCT, BHP, etc.) can be represented as the following vectors:

$$d_j = [d_{1j}, d_{2j}, \dots, d_{N_d j}]^T \in R^{N_d}, \\ d_{obsj} = [d_{obs1j}, d_{obs2j}, \dots, d_{obsN_d j}]^T \in R^{N_d}, \quad (13)$$

where N_d is the number of observed data.

The mapping m to d is described as

$$d_j = f(m_j) + \epsilon, \quad (14)$$

where f is a physical model, ϵ is an error rate in measurements.

The mismatch between the responses of the simulator and the observed data can be represented through the objective function (Emerick, 2016; Le et al., 2016):

$$G_{N_d j} = \frac{1}{2N_d} (d_j^i - d_{obsj})^T C_d^{-1} (d_j^i - d_{obsj}), \quad (15)$$

where i is the iteration number, C_d is the measurement error covariance (Emerick, 2016):

$$C_d = \begin{bmatrix} \sigma_1^2 & 0 & \dots & 0 \\ 0 & \sigma_2^2 & & \vdots \\ \vdots & & \ddots & 0 \\ 0 & 0 & & \sigma_{N_d}^2 \end{bmatrix} \in R^{N_d \times N_d}, \quad (16)$$

where σ is the standard deviation of each measurement.

Then, perturbation of each ensemble member observation is made using the inflation coefficients α_i for each iteration with the restriction (Emerick and Reynolds, 2013) $\sum_{i=1}^N \alpha_i^{-1} = 1$:

$$\tilde{d} = d + \sqrt{\alpha_i} C_d^{1/2} z_d, \quad (17)$$

where $z_d \sim N(0, I_{N_d})$.

The ensemble is updated, taking into account (13) as follows (Chen and Oliver, 2010; Burgers et al., 1998):

$$m_j^{i+1} = m_j^i + C_{md}^i (C_{dd}^i + \alpha_i C_d)^{-1} (d_{obsj}^i - d_j^i + \epsilon_j), \quad (18)$$

where C_{dd} is the autocovariance of the simulated data, which has the form

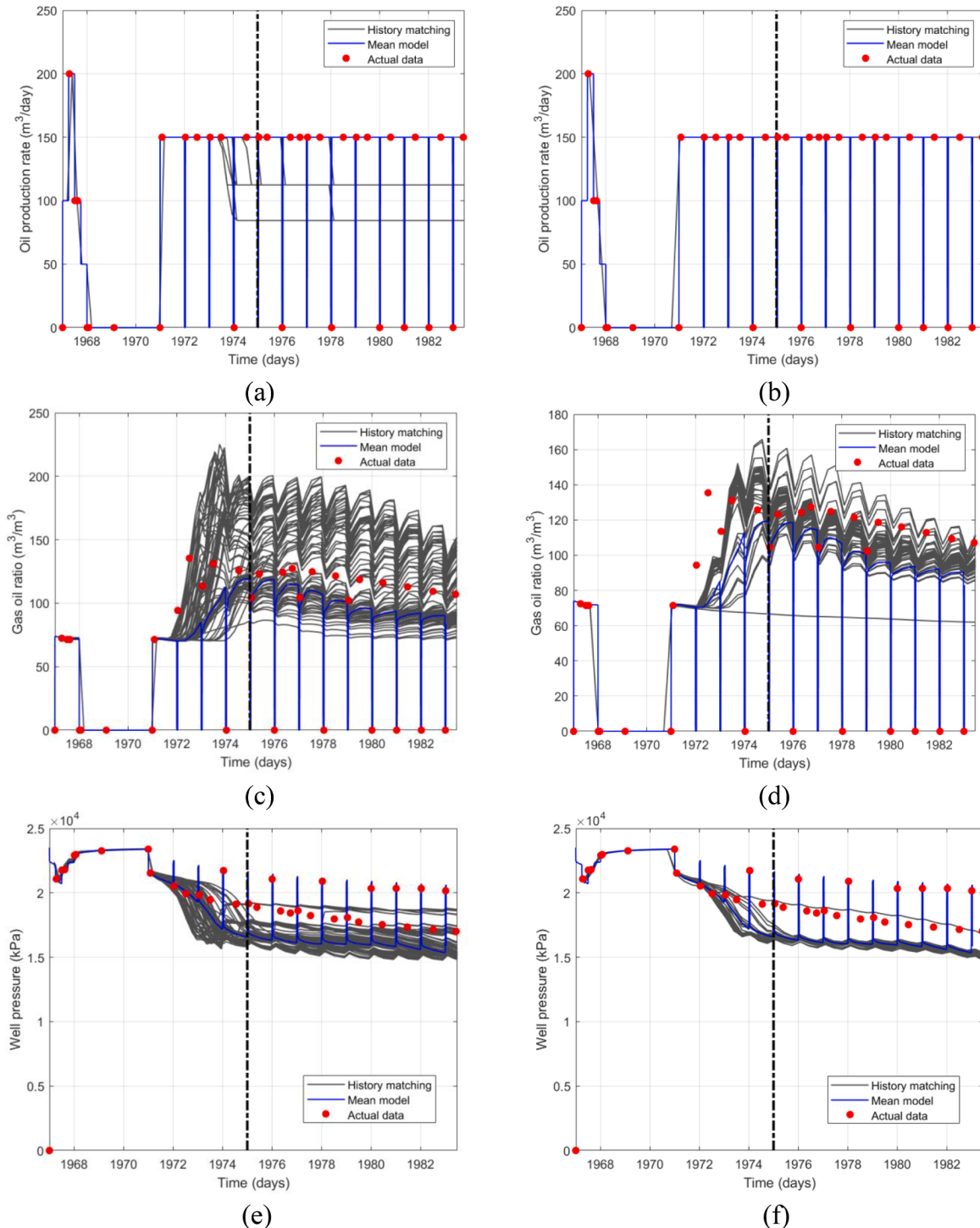


Fig. 11. Production time series for PRO-1 well of the PUNQ-S3 field. Images on the left side represent the prior results and on the right side - the posterior results.

$$C_{dd}^i = \frac{1}{N_e - 1} \sum_{j=1}^{N_e} (d_j^i - \tilde{d}_i) (d_j^i - \tilde{d}_i)^T \in R^{N_d \times N_d}. \quad (19)$$

And C_{md} represents the cross-covariance between parameters of the model and simulated data:

$$C_{md}^i = \frac{1}{N_e - 1} \sum_{j=1}^{N_e} (m_j^i - \tilde{m}_i) (d_j^i - \tilde{d}_i)^T \in R^{N_m \times N_d}. \quad (20)$$

The process is repeated until the convergence condition is satisfied.

4. Experimental reservoir models

4.1. PUNQ-S3

PUNQ-S3 is a reservoir model built based on a real field study of the PUNQ (Production forecasting with UNcertainty Quantification) project (Fig. 3). In the technical literature, PUNQ-S3 was used as a test case for several inverse methods, including EnKF. Therefore, it was considered an ideal experiment candidate (Floris et al., 2001).

The field contains oil and gas. It has six production wells (Table 2).

The model contains five layers with 19×28 grid blocks, 1761 of

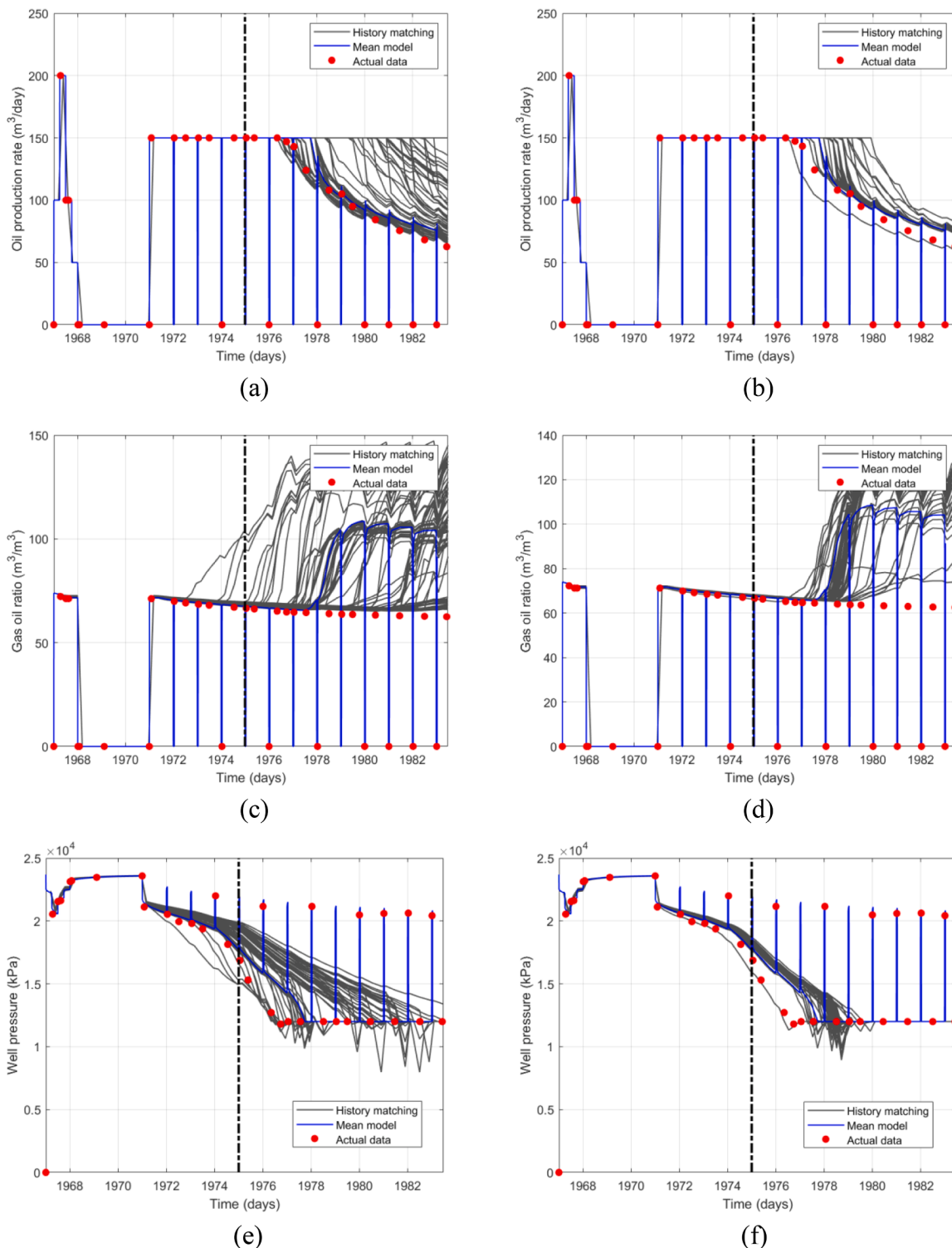


Fig. 12. Production time series for PRO-11 well of the PUNQ-S3 field. Images on the left side represent the prior results and on the right side - the posterior results.

which are active. The size of the horizontal block is $180 \times 180 m^2$. The details of the reservoir model parameters for PUNQ-S3 are shown in Table 3.

Figs. 4, 5, and 6 show porosity (PORO), horizontal (PERMX), and vertical permeability (PERMZ) of each reservoir layer, respectively.

Initially, all six production wells were subjected to an extended test (1 year) followed by a 3-year shut-off and a four year production period (Verga et al., 2013). The drawdown of a well test consisted of four production intervals, each of which lasted three months at a constant

flow rate. For four years, the oil flow rate was set at $150 m^3/day$, and all wells were closed for 2 weeks each year to collect static pressure in the reservoir.

4.2. Volve field

The dataset is provided by a Norwegian multinational energy company called Equinor. The data from the NCS (Norwegian continental shelf) has been available since June 2018 (Johansen et al., 2007; Nagy,

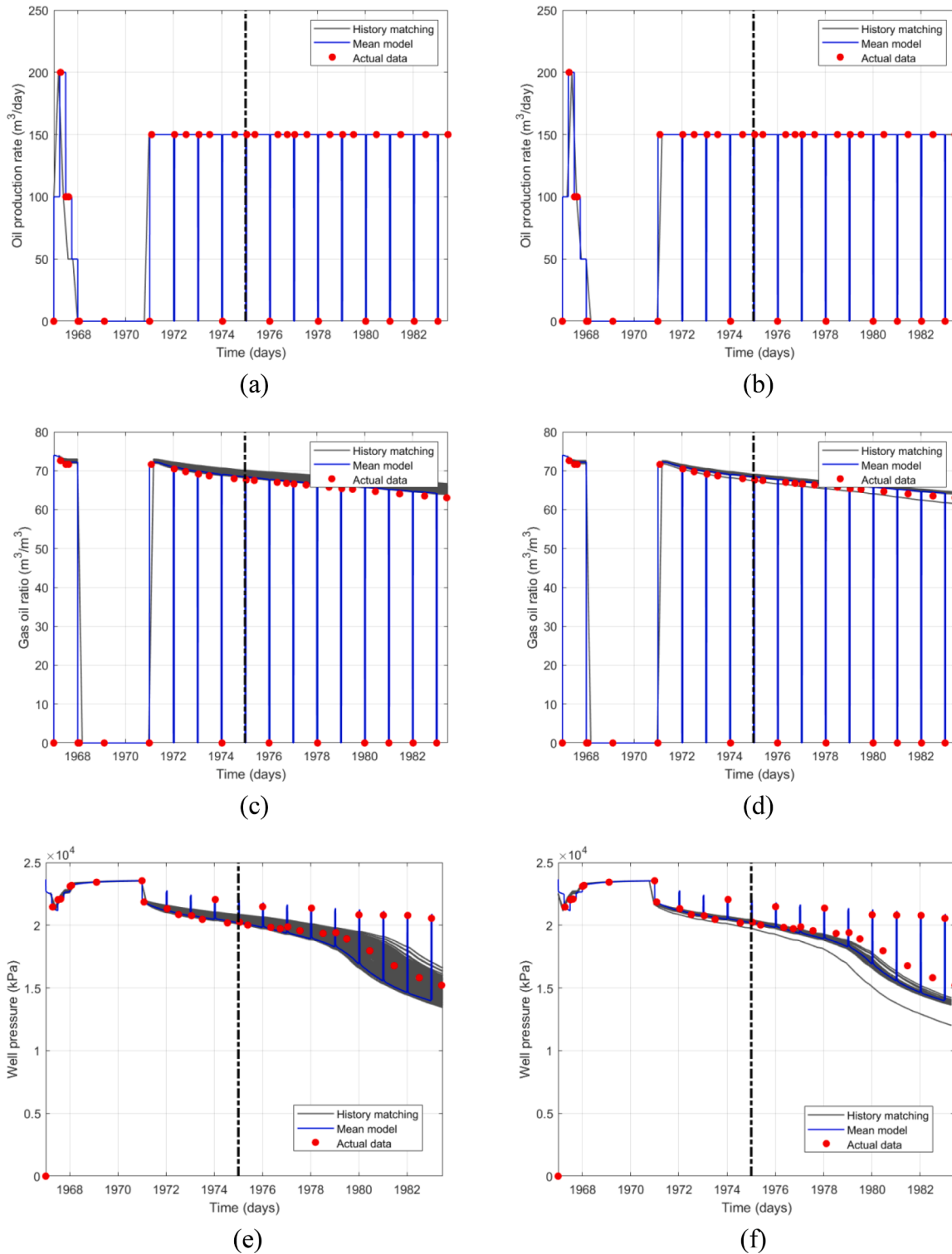


Fig. 13. Production time series for PRO-12 well of the PUNQ-S3 field. Images on the left side represent the prior results and on the right side - the posterior results.

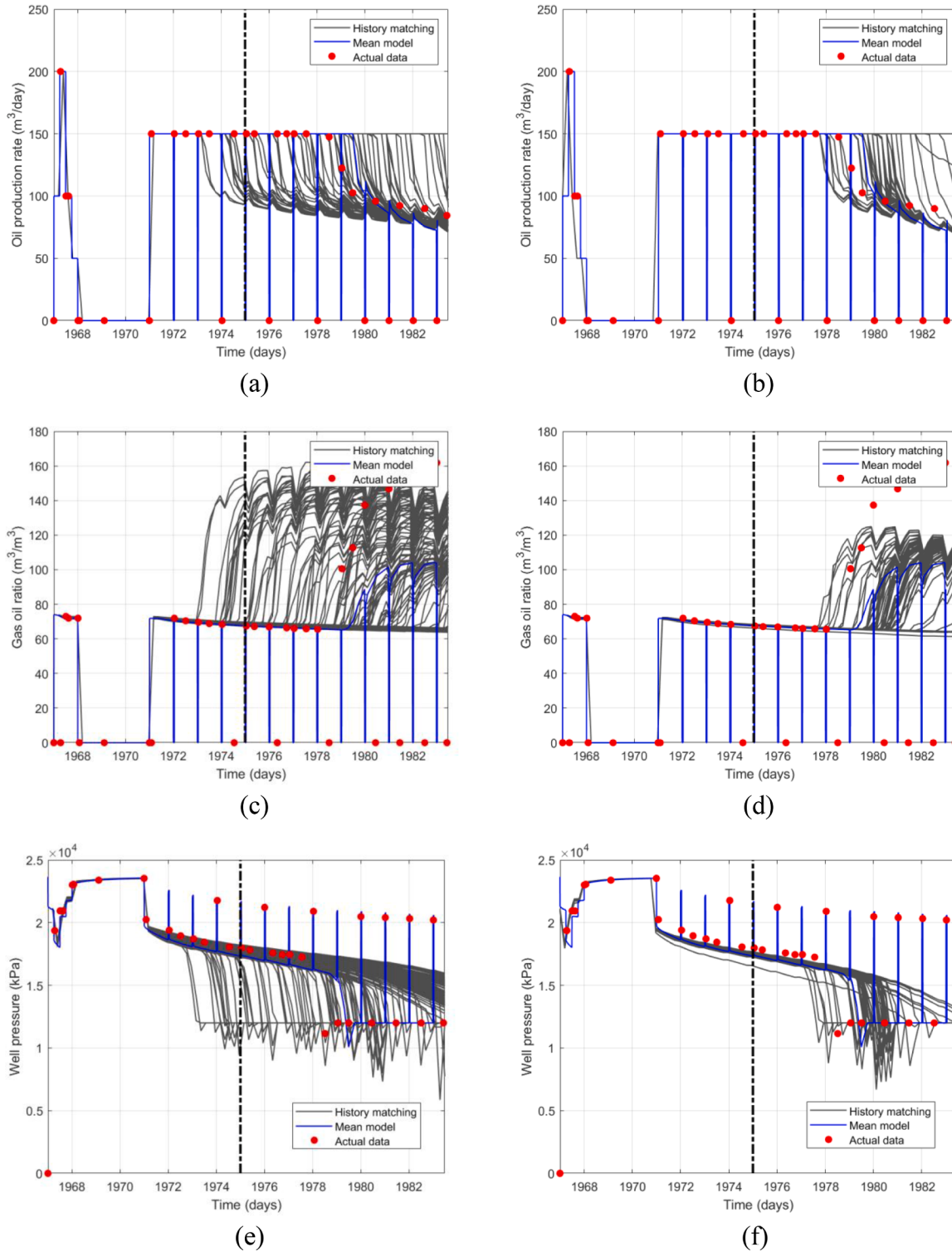


Fig. 14. Production time series for PRO-15 well of the PUNQ-S3 field. Images on the left side represent the prior results and on the right side - the posterior results.

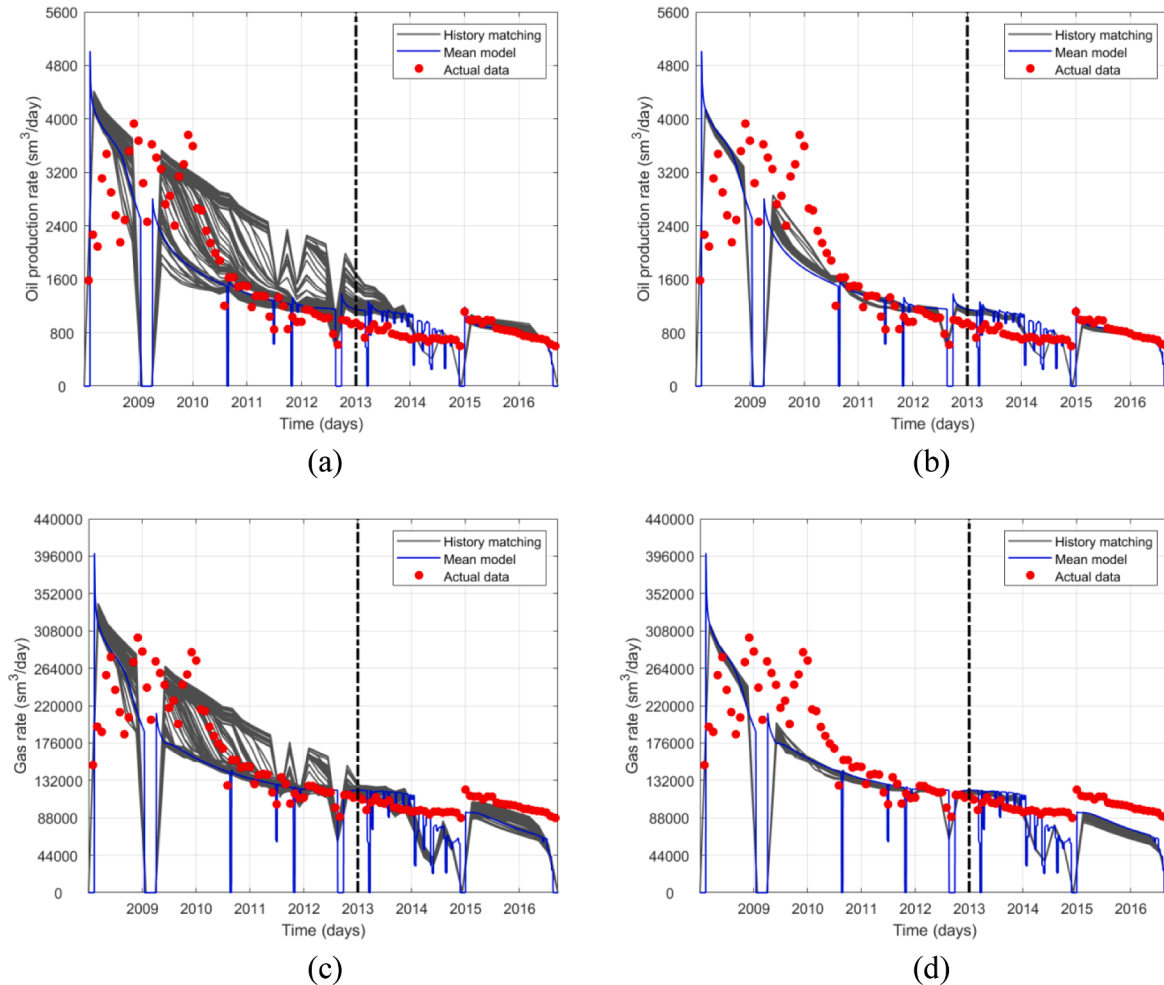


Fig. 15. Production time series for P-F-12 well of the Volvo field. Images on the left side represent the prior results and on the right side - the posterior results.

2019). The Volvo field is a reservoir that operated for 8.5 years until 2016 (Fig. 7).

Volvo field was operated from 2008 to 2016 when it was shut down and decommissioned in 2018 (Volvo dataset, 2018). Table 4 describes the production and injection wells of the Volvo field.

Table 5 lists the parameters of the reservoir model. Figs. 8, 9, and 10 show PORO, PERMX, and PERMZ of each reservoir layer for the Volvo field, respectively.

5. Evaluation metrics

To analyse the performance of the proposed approach, the following metrics are considered: RMSE, R^2 , and MAE.

RMSE shows the difference between real and simulated data and is calculated as

$$RMSE = \sqrt{\frac{1}{N_{obs}} \sum_{i=1}^{N_{obs}} (Y_i - \tilde{Y}_i)^2}, \quad (21)$$

where Y_i is true data, \tilde{Y}_i is simulated data and N_{obs} is the number of observations.

R^2 is a statistical measure that relates the proportion of a change in a dependent variable, which is explained by an independent variable, using regression analysis.

$$R^2 = 1 - \frac{\sum_{i=1}^{N_{obs}} (Y_i - \tilde{Y}_i)^2}{\sum_{i=1}^{N_{obs}} (Y_i - \bar{Y})^2}, \quad (22)$$

where \bar{Y} is a mean value of Y .

MAE represents the average absolute value of errors and is calculated as

$$MAE = \frac{1}{N_{obs}} \sum_{i=1}^{N_{obs}} |Y_i - \tilde{Y}_i|. \quad (23)$$

6. Experimental results

In the paper, the reservoir modeling experiments are performed in CMG IMEX, CMG CMOST, and MATLAB Reservoir Simulation Toolbox (MRST) (Lie et al., 2012). All experiments were conducted on Intel Xeon®, CPU X5670 @ 2.93 GHz × 4 with 10 GB of machine RAM.

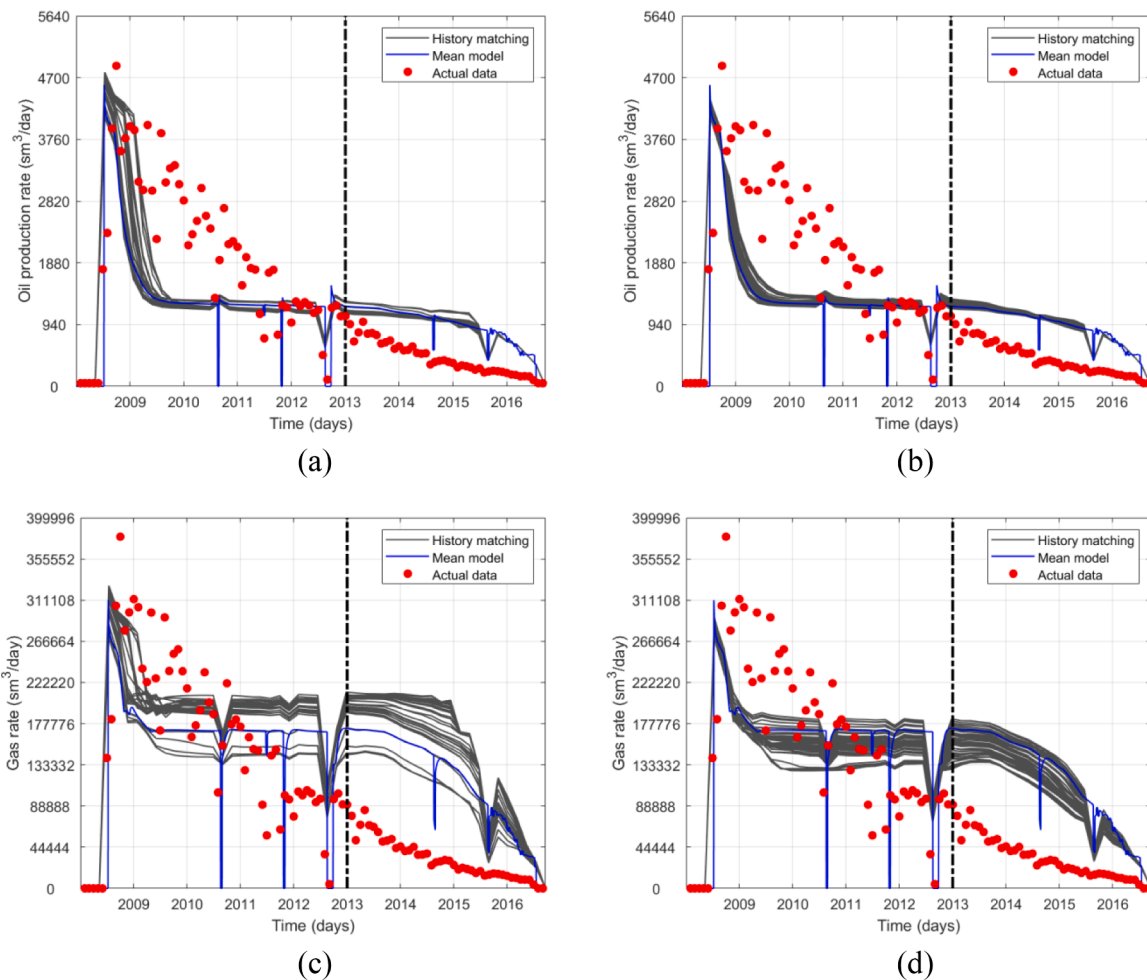


Fig. 16. Production time series for P-F-14 well of the Volvo field. Images on the left side represent the prior results and on the right side - the posterior results.

ConvBiGRU-VAE training was conducted in Python 2.7.13 using various libraries, including Tensorflow and Keras, over 100 epochs (full cycles of stochastic gradient descent).

To evaluate the method, we generate a synthetic dataset of 2000 realizations using the SKUA-GOCAD software. Then, we generate the realizations of the reservoir permeability and porosity from ConvBiGRU-VAE, which make up the original ensemble. In this case, only the geological distribution changes in each realization, keeping the modeling data unchanged. The realizations datasets are split into 80% training data and 20% test data for ConvBiGRU-VAE validation. ConvBiGRU-VAE is trained using RMSE as a loss function to validate the reconstructed images with the initial dataset. The images are then compressed. In the next step, they go through the decoder, where they are reconstructed. The ensemble average of models is a model with spatially invariant porosity and permeability.

The optimal ensemble size was experimentally estimated and was equal to 100.

The effectiveness of the proposed approach for history matching is estimated using reservoir well time series for the parameters of the a priori and posterior models. Figs. 11–14 shows the time series for PUNQ-S3 wells, where the gray lines represent the ensemble members, the blue

line represents the mean model, and the red dots represent the observed data. The black vertical dashed line for 3000 days in Figs. 11–14 separates the phases of assimilation and prediction. It should be noted that for PUNQ-S3 model, PRO-1, PRO-11, PRO-12, and PRO-15 wells are selected randomly.

An attempt at GOR comparison after 1975 led to a slight deterioration in the results from 1975 to 1983 for PRO-11 and PRO-15 wells. The figure shows very close agreement with the observed data for 3000 days. There is also a decrease in uncertainty of oil rate and BHP for PRO-1, PRO-11, and PRO-15 wells (Figs. 11, 12, 13, respectively).

Thus, despite the forecast uncertainty, the history matching results for PUNQ-S3 wells were significantly improved, according to accuracy and variance.

The experiments were conducted on two randomly selected producer wells (P-F-12 and P-F-14) for the Volvo field. According to Figs. 15 and 16, the dashed vertical line between assimilation and forecasting phases passes through 2013.

The proposed approach shows good results for oil rate and gas rate for P-F-14 well (Fig. 16). However, the performance of the predicted distributions is poor compared to the results for P-F-12 (Fig. 15).

Also, Fig. 15 demonstrates similar distributions with the reference

Table 6
Performance evaluation of the proposed approach for PUNQ-S3.

Well	Data	Evaluation metric	Initial	EnKF	Proposed approach
PRO-1	Oil rate	RMSE	52.9133	25.9426	17.7636
		R ²	0.5204	0.9347	0.9652
		MAE	30.8367	18.1452	7.2066
	GOR	RMSE	100.0445	36.3470	34.4983
		R ²	0.5517	0.7409	0.9042
		MAE	60.4169	24.0954	22.1117
	BHP	RMSE	107.4441	90.5177	54.2768
		R ²	0.5803	0.8116	0.9815
		MAE	67.0001	55.5902	35.5017
	Oil rate	RMSE	22.5007	19.8421	18.8590
		R ²	0.5110	0.9195	0.9234
		MAE	12.6568	8.7485	8.0850
	GOR	RMSE	29.4307	18.1566	25.5885
		R ²	0.7439	0.8518	0.7804
		MAE	15.6601	9.8634	13.1419
	BHP	RMSE	63.1400	52.2537	57.3558
		R ²	0.6287	0.9618	0.8895
		MAE	36.7409	27.7445	29.3681
PRO-11	Oil rate	RMSE	1.1405	0.0001	0.0001
		R ²	0.9733	1.0000	1.0000
		MAE	0.8999	0	0
	GOR	RMSE	3.6317	0.9198	0.5843
		R ²	0.9120	0.9999	0.9999
		MAE	0.9905	0.6647	0.4510
	BHP	RMSE	100.0002	94.1918	24.1635
		R ²	0.5318	0.7377	0.9911
		MAE	73.0441	52.6562	14.0614
	Oil rate	RMSE	32.0044	27.7670	24.1338
		R ²	0.7105	0.8353	0.8717
		MAE	18.0311	12.5607	10.1350
	GOR	RMSE	30.0601	20.8058	26.2164
		R ²	0.6083	0.6909	0.6909
		MAE	19.6296	10.3037	11.7111
	BHP	RMSE	27.1900	1.9052	1.7823
		R ²	0.7505	0.9072	0.8745
		MAE	15.7142	1.0715	0.8727

Table 7
Performance evaluation of the proposed approach for Volvo field.

Well	Data	Evaluation metric	Initial	EnKF	Proposed approach
P-F-12	Oil rate	RMSE	116.1665	19.2583	9.8901
		R ²	0.9175	0.9942	0.9986
		MAE	61.2374	10.8349	4.7901
	Gas rate	RMSE	58.8430	10.0891	6.5144
		R ²	0.9383	0.9669	0.9847
		MAE	32.1900	6.7519	3.7216
P-F-14	Oil rate	RMSE	53.3881	19.8192	15.7552
		R ²	0.9495	0.9882	0.9922
		MSE	19.7581	10.0150	7.1682
	Gas rate	RMSE	5.3755	3.3641	2.1855
		R ²	0.9067	0.9849	0.9962
		MAE	1.7635	1.8144	1.3909

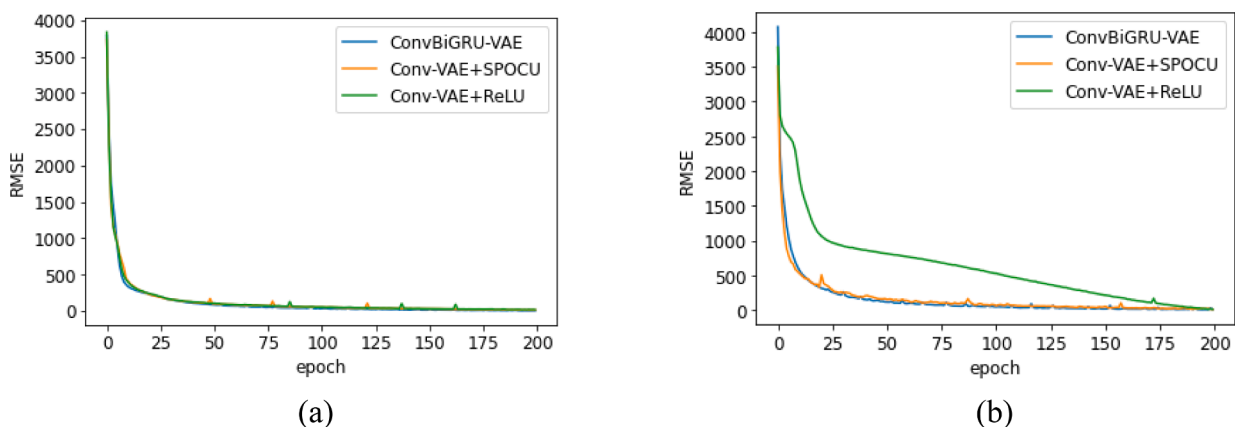


Fig. 17. Loss curves for ConvBiGRU-VAE model.

case for oil rate and gas rate. However, the oil rate gives the best results. For the Volvo field, this proves the ability of the proposed approach to reproduce the truth with acceptable uncertainty in the reservoir model.

The results show that the extracted features can capture the characteristics of the reservoir. The forecast results from the adopted implementations provide a relatively accurate assessment of production characteristics.

7. Discussions

This section discusses the experimental results obtained using the ConvBiGRU-VAE model.

The posterior results show a significant reduction in the variance of the resulting ensemble members compared to the initial ensemble members for PRO-12 well (Fig. 13).

Tables 6 and 7 show the performance comparison of the proposed approach with EnKF according to the MAE, RMSE, and R² metrics for PUNQ-S3 and Volvo fields, respectively.

We obtained realizations from production data better than the EnKF algorithm.

Fig. 17 shows training loss curves for PUNQ-S3 and Volvo field. The ConvBiGRU-VAE model is compared with the convolutional VAE using the ReLU activation function (Conv-VAE+ReLU) and convolutional VAE based on SPOCU (Conv-VAE+SPOCU).

Experiments for the PUNQ-S3 field model record RMSE values averaging 9.8710, 12.1376 and 16.7653 for ConvBiGRU-VAE, Conv-VAE+SPOCU and Conv-VAE+ReLU, respectively (Fig. 17 (a)). Whereas for the Volvo field, they averaged 7.2695, 8.8758, and 9.2779, respectively (Fig. 17 (b)). The blue curve corresponding to ConvBiGRU-VAE showed the best performance for both cases.

Overall, the history matching results for the PUNQ-S3 and Volvo fields were reasonably accurate.

8. Conclusions

In this paper, an approach was developed to history assimilation using deep learning. ConvBiGRU-VAE was considered to generate and fine-tune the porosity and permeability parameters that were used to train the reservoir model. The proposed model combined the advantages of AlexNet and BiGRU. SPOCU was considered as the activation function. Then the model parameters were updated using ES-MDA. It allows for a more accurate assessment of the reservoir model and forecasting of future production rates. This methodology was applied to the analysis of PUNQ-S3 and Volve fields. The proposed approach was compared with EnKF, Conv-VAE+ReLU, and Conv-VAE+SPOCU. The ability of the proposed approach to reproduce the truth with acceptable uncertainty in the reservoir model for the considered oil fields was observed. The most accurate result showed the proposed approach based on ConvBiGRU-VAE. The study shows the potential for applying the proposed method in automatic history matching.

CRediT authorship contribution statement

Rasim Alguliyev: Conceptualization, Investigation, Methodology, Validation, Writing – review & editing. **Ramiz Alguliyev:** Conceptualization, Investigation, Methodology, Validation, Writing – review & editing, Visualization. **Yadigar Imamverdiyev:** Conceptualization, Investigation, Methodology, Validation, Writing – review & editing, Visualization. **Lyudmila Sukhostat:** Conceptualization, Investigation, Methodology, Validation, Writing – review & editing, Visualization.

Declaration of Competing Interest

The authors declare that they have no known competing financial interests or personal relationships that could have appeared to influence the work reported in this paper.

Acknowledgments

This work was supported by the Science Foundation of the State Oil Company of Azerbaijan Republic (SOCAR) (Contract No. 3LR-AMEA). The authors want to thank Dr. Olwijn Leeuwenburgh and Dr. Dries Hegen from TNO (Netherlands) for providing us the EnKF module for MRST.

References

- Burgers, G., van Leeuwen, P. J., & Evensen, G. (1998). Analysis scheme in the ensemble Kalman filter. *Monthly Weather Review*, 126(6), 1719–1724. [https://doi.org/10.1175/1520-0493\(1998\)126%3c1719:ASITEK%3e2.0.CO;2](https://doi.org/10.1175/1520-0493(1998)126%3c1719:ASITEK%3e2.0.CO;2)
- Canchumuni, S. A., Emerick, A. A., & Pacheco, M. A. (2017). Integration of ensemble data assimilation and deep learning for history matching facies models. In *Proceedings of the offshore technology conference*. <https://doi.org/10.4043/28015-MS>. October 2017.
- Canchumuni, S. A., Emerick, A. A., & Pacheco, M. (2018). History matching channeled facies models using ensemble smoother with a deep learning parameterization. In *Proceedings of the ECMOR XVI - 16th European conference on the mathematics of oil recovery* (pp. 3–6). <https://doi.org/10.3997/2214-4609.201802277>. September.
- Canchumuni, S. W. A., Emerick, A. A., & Pacheco, M. A. C. (2019). Towards a robust parameterization for conditioning facies models using deep variational autoencoders and ensemble smoother. *Computers & Geosciences*, 128, 87–102. <https://doi.org/10.1016/j.cageo.2019.04.006>
- Chen, Y., & Oliver, D. S. (2014). History matching of the Norne full-field model using an iterative ensemble smoother. *SPE Reservoir Evaluation & Engineering*, 17(2), 244–256. <https://doi.org/10.2118/0414-0119-JPT>
- Chen, Y., & Oliver, D. S. (2010). Ensemble-based closed-loop optimization applied to Brugge field. *SPE Reservoir Evaluation & Engineering*, 13, 56–71. <https://doi.org/10.2118/118926-PA>
- Chen, Z., Yeo, C. K., Lee, B. S., Lau, C. T., & Jin, Y. (2018). Evolutionary multi-objective optimization based ensemble autoencoders for image outlier detection. *Neurocomputing*, 309, 192–200. <https://doi.org/10.1016/j.neucom.2018.05.012>
- Cho, K., Van Merriënboer, B., Gulcehre, C., Bahdanau, D., Bougares, F., Schwenk, H., & Bengio, Y. (2014). Learning phrase representations using RNN encoder-decoder for statistical machine translation. In *Proceedings of the international conference on SIGDAT*. <https://doi.org/10.3115/v1/D14-1179>
- Emerick, A. A. (2016). Analysis of the performance of ensemble based assimilation of production and seismic data. *The Journal of Petroleum Science and Engineering*, 139, 219–239. <https://doi.org/10.1016/j.petrol.2016.01.029>
- Emerick, A. A., & Reynolds, A. C. (2013). Ensemble smoother with multiple data assimilation. *Computers & Geosciences*, 55, 3–15. <https://doi.org/10.1016/j.cageo.2012.03.011>
- Esen, H., Inalli, M., Sengur, A., & Esen, M. (2008a). Artificial neural networks and adaptive neuro-fuzzy assessments for ground-coupled heat pump system. *Energy and Buildings*, 40(6), 1074–1083. <https://doi.org/10.1016/j.enbuild.2007.10.002>
- Esen, H., Inalli, M., Sengur, A., & Esen, M. (2008b). Forecasting of a ground-coupled heat pump performance using neural networks with statistical data weighting pre-processing. *International Journal of Thermal Sciences*, 47(4), 431–441. <https://doi.org/10.1016/j.ijthermalsci.2007.03.004>
- Esen, H., Inalli, M., Sengur, A., & Esen, M. (2008c). Performance prediction of a ground-coupled heat pump system using artificial neural networks. *Expert Systems with Applications*, 35(4), 1940–1948. <https://doi.org/10.1016/j.eswa.2007.08.081>
- Esen, H., Ozgen, F., Esen, M., & Sengur, A. (2009). Artificial neural network and wavelet neural network approaches for modelling of a solar air heater. *Expert Systems with Applications*, 36(8), 11240–11248. <https://doi.org/10.1016/j.eswa.2009.02.073>
- Esen, H., Esen, M., & Ozsolak, O. (2017). Modelling and experimental performance analysis of solar-assisted ground source heat pump system. *Journal of Experimental and Theoretical Artificial Intelligence*, 29(1), 1–17. <https://doi.org/10.1080/0952813X.2015.1056242>
- Evensen, G. (1994). Sequential data assimilation with a nonlinear quasi-geostrophic model using Monte Carlo methods to forecast error statistics. *Journal of Geophysical Research*, 99(C5), 10143–10162. <https://doi.org/10.1029/94JC00572>
- Evensen, G. (2003). The ensemble Kalman filter: Theoretical formulation and practical implementation. *Ocean Dynamics*, 53, 343–367. <https://doi.org/10.1007/s10236-003-0036-9>
- Feng, S., & Duarte, M. F. (2018). Graph autoencoder-based unsupervised feature selection with broad and local data structure preservation. *Neurocomputing*, 312, 310–323. <https://doi.org/10.1016/j.neucom.2018.05.117>
- Floris, F. J. T., Bush, M. D., Cuypers, M., Roggero, F., & Syversveen, A. R. (2001). Methods for quantifying the uncertainty of production forecasts: A comparative study. *Petroleum Geoscience*, 7(S), S87–S96. <https://doi.org/10.1144/petgeo.7.S.S87>
- Furrer, R., & Bengtsson, T. (2007). Estimation of high-dimensional prior and posterior covariance matrices in Kalman filter variants. *Journal of Multivariate Analysis*, 98(2), 227–255. <https://doi.org/10.1016/j.jmva.2006.08.003>
- Gao, Z., Li, Z., Luo, J., & Li, X. (2022). Short-text aspect-based sentiment analysis based on CNN + BiGRU. *Applied Sciences*, 12(5), 2707. <https://doi.org/10.3390/app12052707>
- Gilman, J. R., & Ozgen, C. (2013). *Reservoir simulation: History matching and forecasting*. United States: Society of Petroleum Engineers.
- Hajizadeh, Y., Christie, M., & Demyanov, V. (2011). Ant colony optimization for history matching and uncertainty quantification of reservoir models. *Journal of Petroleum Science and Engineering*, 77(1), 78–92. <https://doi.org/10.1016/j.petrol.2011.02.005>
- Isaiah, J., Schrader, S., Reichhardt, D., & Link, C. (2013). Performing reservoir simulation with neural network enhanced data. In *Proceedings of the SPE digital energy conference* (pp. 5–7). <https://doi.org/10.2118/163691-MS>. March.
- Johansen, A., Kveinen, E., Byberg, G.O., Lehne, K.A., Skeide, M., Solymar, S., Ostensen, S., Nesse, T., Berge, T.H., 2007. Volve field – Recommendation to drill well NO 15/9-F-7 and Well NO 15/9-F-9, Statoil.
- Kim, J., Kang, B., Jeong, H., & Choe, J. (2019). Field development optimization using a cooperative micro-particle swarm optimization with parameter integration schemes. *Journal of Petroleum Science and Engineering*, 183, 1–14. <https://doi.org/10.1016/j.petrol.2019.106416>
- Kim, J., Park, C., Ahn, S., Kang, B., Jung, H., & Jang, I. (2021). Iterative learning-based many-objective history matching using deep neural network with stacked autoencoder. *Petroleum Science*, 18(5), 1465–1482. <https://doi.org/10.1016/j.petsci.2021.08.001>
- Kingma, D. P., Salimans, T., & Welling, M. (2015). Variational dropout and the local reparameterization trick. In *Proceedings of the 29th annual conference on neural information processing systems (NIPS)* (pp. 5–10). December.
- Kingma, D. P., & Welling, M. (2014). Auto-encoding variational Bayes. In *Proceedings of the international conference on learning representations (ICLR)* (pp. 14–16). April.
- Kiselák, J., Lu, Y., Švihář, J., Szépe, P., & Stehlík, M. (2021). SPOCU: Scaled polynomial constant unit activation function. *Neural Computing and Applications*, 33, 3385–3401. <https://doi.org/10.1007/s00521-020-05182-1>
- Krizhevsky, A., Sutskever, I., & Hinton, G. (2012). Imagenet classification with deep convolutional networks. *Communications of the ACM*, 60(6), 84–90. <https://doi.org/10.1145/3065386>
- Le, D. H., Emerick, A. A., & Reynolds, A. C. (2016). An adaptive ensemble smoother with multiple data assimilation for assisted history matching. *SPE Journal*, 21(6), 2195–2207. <https://doi.org/10.2118/173214-PA>
- Li, H., & Yang, D. (2012). Estimation of multiple petrophysical parameters for hydrocarbon reservoirs with the ensemble-based technique. *Petroleum Exploration and Development*, 4(2), 1–17. <https://doi.org/10.3968/j.aped.1925543820120402.812>
- Lie, K. A., Krogstad, S., Ligaarden, I. S., Natvig, J. R., Nilsen, H. M., & Skaflestad, B. (2012). Open-source MATLAB implementation of consistent discretisations on complex grids. *Computers & Geosciences*, 16(2), 297–322. <https://doi.org/10.1007/s10596-011-9244-4>
- Liu, M., & Grana, D. (2018). Ensemble-based seismic history matching with data re-parameterization using convolutional autoencoder. In *Proceedings of the SEG international exposition and 88th annual meeting*. <https://doi.org/10.1190/segam2018-2997988.1>, 14–19 October.

- Liu, Y., Sun, W., & Durlofsky, L. J. (2019). A deep-learning-based geological parameterization for history matching complex models. *Mathematical Geosciences*, 51, 725–766. <https://doi.org/10.1007/s11004-019-09794-9>
- Lorentzen, R. J., Luo, X., Bhakta, T., & Valestrand, R. (2019). History matching the full Norne field model using seismic and production data. *SPE Journal*, 24(04), 1–16. <https://doi.org/10.2118/194205-PA>
- Luo, X., Stordal, A. S., & Lorentzen, R. J. (2015). Iterative ensemble smoother as an approximate solution to a regularized minimum-average-cost problem: Theory and applications. *SPE Journal*, SPE-176023-PA 20(5), 962–982. <https://doi.org/10.2118/176023-PA>
- Ma, Y. Z. (2019). *Quantitative geosciences: Data analytics, geostatistics, reservoir characterization and modeling*. Switzerland: Springer Nature. <https://doi.org/10.1007/978-3-030-17860-4>
- Mohamed, L., Christie, M. A., Demyanov, V., Robert, E., & Kachuma, D. (2010). Application of particle swarms for history matching in the Brugge reservoir. In *Proceedings of the SPE annual technical conference and exhibition*. <https://doi.org/10.2118/135264-MS>, 19–22 September.
- Mohd Razak, S., & Jafarpour, B. (2020). Convolutional neural networks (CNN) for feature-based model calibration under uncertain geologic scenarios. *Computers & Geosciences*, 24, 1625–1649. <https://doi.org/10.1007/s10596-020-09971-4>
- Nagy, A. (2019). Availability and Quality of Drilling Data in the Volve Dataset. University of Stavanger, Norway. Master's thesis. https://uis.brage.unit.no/uis-xmlui/bitstream/handle/11250/2634139/Nagy_Attila.pdf.
- Negash, B. M., Ayoub, M. A., Jufar, S. R., & Robert, A. J. (2017). History matching using proxy modeling and multiobjective optimizations. Awang, M., Negash, B., Md Akhir, N., Lubis, L., Md. Rafeek, A.. In *Proceedings of the ICIPETG, international conference on integrated petroleum engineering and geosciences* (pp. 3–16). https://doi.org/10.1007/978-981-10-3650-7_1
- Nikitin, N. O., Revin, I., Hvatov, A., Vychuzhanin, P., & Kalyuzhnaya, A. V. (2022). Hybrid and automated machine learning approaches for oil fields development: The case study of Volve field, North Sea. *Computers & Geosciences*, 161, Article 105061. <https://doi.org/10.1016/j.cageo.2022.105061>
- Nishizaki, H. (2017). Data augmentation and feature extraction using variational autoencoder for acoustic modeling. In *Proceedings of the APSIPA annual summit and conference* (pp. 12–15). <https://doi.org/10.1109/APSIPA.2017.8282225>, December.
- Oliver, D. S., Reynolds, A. C., & Liu, N. (2008). *Inverse theory for petroleum reservoir characterization and history matching*. United Kingdom: Cambridge University Press. <https://doi.org/10.1017/CBO97805115355642>
- Rana, S., Ertekin, T., & King, G. R. (2018). An efficient assisted history matching and uncertainty quantification workflow using Gaussian processes proxy models and variogram based sensitivity analysis: GP-VARS. *Computers & Geosciences*, 114, 73–83. <https://doi.org/10.1016/j.cageo.2018.01.019>
- Ranazzi, P. H., & Sampaio, M. A. (2019a). Ensemble size investigation in adaptive ESMDA reservoir history matching. *The Journal of the Brazilian Society of Mechanical Sciences*, 41, 1–11. <https://doi.org/10.1007/s40430-019-1935-0>
- Ranazzi, P. H., & Sampaio, M. A. (2019b). Influence of the Kalman gain localization in adaptive ensemble smoother history matching. *Journal of Petroleum Science and Engineering*, 179, 244–256. <https://doi.org/10.1016/j.petrol.2019.04.079>
- Stordal, A. S., & Lorentzen, R. J. (2014). An iterative version of the adaptive Gaussian mixture filter. *Computers & Geosciences*, 18, 579–595. <https://doi.org/10.1007/s10596-014-9402-6>
- Tavassoli, Z., Carter, J. N., & King, P. R. (2004). Errors in history matching. *SPE Journal*, 9(3), 352–361. <https://doi.org/10.2118/86883-PA>
- van Leeuwen, P. J., & Evensen, G. (1996). Data assimilation and inverse methods in terms of a probabilistic formulation. *Monthly Weather Review*, 124, 2898–2913. [https://doi.org/10.1175/1520-0493\(1996\)124%3C2898:DAAIMI%3E2.0.CO;2](https://doi.org/10.1175/1520-0493(1996)124%3C2898:DAAIMI%3E2.0.CO;2)
- Verga, F., Cancelliere, M., & Viberti, D. (2013). Improved application of assisted history matching techniques. *Journal of Petroleum Science and Engineering*, 109, 327–347. <https://doi.org/10.1016/j.petrol.2013.04.021>
- Volve dataset. (2018). Volve data village. Equinor. <https://data.equinor.com/dataset/Volve>. [Accessed: 28.05.2020].
- Zhang, K., Lu, R., Zhang, L., Zhang, X., Yao, J., Li, R., & Zhao, H. (2016). A two-stage efficient history matching procedure of non-Gaussian fields. *Journal of Petroleum Science and Engineering*, 138, 189–200. <https://doi.org/10.1016/j.petrol.2015.11.038>